Application of Isothermal Titration Calorimetry in Bioinorganic Chemistry

Nicholas E. Grossoehme • Anne M. Spuches • Dean E. Wilcox

N. E. Grossoehme • A. M. Spuches • D. E. Wilcox (envelope)
Department of Chemistry
6128 Burke Laboratory
Dartmouth College,
Hanover, NH 03755 USA
Email: dwilcox@dartmouth.edu

Present Address:
N. E. Grossoehme
Department of Chemistry
Winthrop University
Rock Hill, SC 29733 USA

Present Address:
A. M. Spuches
Department of Chemistry
East Carolina University
Greenville, NC 27858 USA

Abstract

The thermodynamics of metals ions binding to proteins and other biological molecules can be measured with isothermal titration calorimetry (ITC), which quantifies the binding enthalpy ($\Delta H°$) and generates a binding isotherm. A fit of the isotherm provides the binding constant (K), thereby allowing the free energy ($\Delta G°$) and ultimately the entropy ($\Delta S°$) of binding to be determined. The temperature dependence of $\Delta H°$ can then provide the change in heat capacity ($\Delta C_p°$) upon binding. However, ITC measurements of metal binding can be compromised by undesired reactions (e.g., precipitation, hydrolysis, redox), and generally involve competing equilibria with the buffer and protons, which contribute to the experimental values (K_{ITC}, ΔH_{ITC}). Guidelines and factors that need to be considered for ITC measurements involving metal ions are outlined. A general analysis of the experimental ITC values that accounts for the contributions of metal-buffer speciation and proton competition and provides condition-independent thermodynamic values (K, $\Delta H°$) for metal binding is developed and validated.

Key Words calorimetry • enthalpy • thermodynamics • heat capacity • binding affinity

Abbreviations

ITC	isothermal titration calorimetry
DTT	1,4-dithiothreitol
TCEP	tris(2-carboxyethyl)phosphine
trien	triethylenetetramine
Tris	tris(hydroxymethyl)aminomethane
MOPS	3-morpholinopropanesulfonic acid
ACES	N-(2-acetamido)-2-aminoethanesulfonic acid

Introduction

The thermodynamics of metal ions binding to proteins and other macromolecules is important in many areas of metallobiochemistry, including essential metal trafficking (uptake, transport and delivery), metal-regulated pathways (e.g., metal-dependent transcription factors), enzymes with metal substrates, and the sequestration and removal of toxic metals. Fundamental understanding of these processes requires not only the affinity of the protein for the metal but also the enthalpic and entropic contributions to the free energy of binding.

While the binding constant (K), and thus the change in free energy ($\Delta G°$), can be determined with a variety of methods (e.g., equilibrium dialysis, UV-vis absorption), the key to quantifying the binding thermodynamics is measuring the binding enthalpy ($\Delta H°$)[1]. While the van't Hoff relationship allows $\Delta H°$ to be determined from the temperature-dependence of K, this provides an average value over the experimental temperature range and $\Delta H°$ varies with temperature when binding affects the heat capacity, resulting in a significant value of $\Delta C_p°$, as is often the case with proteins. Calorimetry directly measures the binding enthalpy under isobaric conditions ($q_p = \Delta H°$), allowing the binding entropy ($\Delta S°$) to be determined from the fundamental thermodynamic relationship, $\Delta G° = \Delta H° - T\Delta S°$. Finally, $\Delta C_p°$, can be determined from the temperature-dependence of $\Delta H°$, based on the relationship $\Delta C_p° = \Delta\Delta H°/\Delta T$.

Due to the development of sensitive titration microcalorimeters [1, 2], the technique of isothermal titration calorimetry (ITC) has become widely used to quantify binding constants and thermodynamics in biochemical and biophysical studies [3], including those involving metal ions [4]. The heat flow from sequential injections of one binding partner (e.g., metal ion) into a cell containing the other binding partner (e.g., protein) is integrated and normalized for concentration to generate a binding isotherm (Figure 1), which depends on the stoichiometry (*n*), binding constant (K_{ITC}) and change in enthalpy (ΔH_{ITC}).

Titration calorimeters, however, measure the sum of the heat associated with *all* processes occurring upon addition of aliquots of the titrant. This necessarily includes the heat of dilution of the titrant, but also the heat associated with any undesired reactions, such as precipitation, hydrolysis and redox in the case of metal ions, as well as any equilibria that are

---

[1] Titration calorimeters typically operate at constant ambient pressure (~1 atm), but solute concentrations are normally far from standard values. Nevertheless, the superscript naught is typically used with thermodynamic parameters obtained from ITC measurements.

intrinsically coupled to the desired binding equilibrium. The issues of competing and multiple equilibria are well known for complexometric titrations (e.g., EDTA titrations of metal ions) with a variety of methods (spectrophotometry, electrochemistry, etc.) [5], and accurate information about the equilibrium of interest requires accounting for any intrinsic competing equilibria.

The binding isotherm from an ITC thermogram quantifies the amount of complex that is formed over the course of a titration by measuring its heat of formation. As is well known for a variety of techniques that quantify metal-complex formation based on other physical properties, the isotherm is fit to obtain a binding constant, which is practically limited in ITC to the range $\sim10^3 < K < \sim10^8$ (1 mM > K_d > 10 nM). The conditions that define these limits can be estimated by the parameter c, where $c = n$ K [macromolecule] and $\sim1 < c < \sim1000$ (ideally $5 < c < 500$) indicates the range over which a unique fit of the ITC data may be obtained [1]. Figure 2 indicates the shape[2] of the binding isotherm over this range, from a broad shallow curve at low c to a step at high c; outside of this c window, ITC data can only indicate an upper or lower limit for K, respectively. However, careful measurements can extend the lower limit when the binding stoichiometry is known [6], and the upper limit can be extended by including a known competing ligand.

Fitting the ITC binding isotherm to an appropriate model (independent binding sites, sequential binding sites, etc.) provides values of n, K_{ITC} and ΔH_{ITC} for one or more sites (Fig. 1). For the simple case of 1:1 binding ($n = 1$) with no competing equilibria, the desired thermodynamic parameters (K, $\Delta H°$) are obtained directly from the best fit of the data. However, competing equilibria are commonly associated with metal coordination chemistry, and subsequent analysis of K_{ITC} and ΔH_{ITC} is generally required to obtain K and $\Delta H°$, as described below. While inorganic and bioinorganic chemists are generally aware of coupled binding equilibria, those who have less experience working with metal ions may not appreciate their impact on the measurement of metal binding by ITC and other methods.

Common and specific challenges are found with ITC measurements involving metal ions, many of which were considered in early studies of Fe^{3+} binding to tranferrin [7, 8]. Specific to ITC are issues associated with the measurement of heat flow, which contains contributions from

---

[2] Hyperbolic or sigmoidal shapes of ITC binding isotherms do not reflect the absence or presence of cooperative binding.

any undesired reactions and/or competing equilibria, and accurate determination of the binding enthalpy. As is well known for metal binding studies in buffered aqueous solutions, there is an inevitable interaction between the metal ion (Lewis acid) and the buffer (Lewis base), which is present in large excess; this ranges from small, though rarely negligible, to dominant (e.g., $\log \beta_4$ = 14.1 for $Cu(Tris)_4^{2+}$) [9]. Since buffer competition with the macromolecule for the metal has an effect on K_{ITC} and ΔH_{ITC} and must be removed in subsequent analysis, both the stability and the enthalpy of formation of metal-buffer complexes under the experimental conditions are required. Another concern is heat associated with precipitation of the metal or the protein, although a precipitate may be observed at the end of the titration and experimental conditions adjusted to maintain solubility. A third concern is hydrolysis reactions of the metal ion. These can lack a visual clue, but evidence may be found in control titrations. Hydrolysis is particularly insidious because it often depends on concentration and there is a significant dilution of the metal when it is injected into the macromolecule solution in the cell (designated metal $\rightarrow$ macromolecule). However, both precipitation and hydrolysis can be suppressed by delivering the metal as a well-defined complex that prevents these undesired heat-producing processes, and a metal-buffer complex can often serve this purpose.

Redox reactions of transition metals are generally an undesirable complication in metal binding studies. Deoxygenated solutions and anaerobic conditions (e.g., placing the calorimeter in an inert atmosphere box) can prevent oxidation and its heat contribution, as can ligands that stabilize the oxidation state of interest. One relevant example is Cu^+, which is readily oxidized and also unstable to disproportionation ($2Cu^+ \rightleftarrows Cu^0 + Cu^{2+}$; $K \approx 10^6$), requiring both anaerobic conditions and a Cu^+-stabilizing ligand to ensure delivery of a known concentration of this ion. While the presence of a reducing agent, such as sodium dithionite, helps to suppress oxidation, its reaction with O_2 contributes to the measured heat and reductants should only serve as a secondary precaution with anaerobic conditions. Further, some metal ions form stable complexes with common reductants, such as DTT [10] and TCEP [11], which may contribute to the experimental binding equilibrium and enthalpy.

Experimental Design
A number of factors should be considered when designing and conducting ITC measurements involving metal ions.

1. Experimental conditions should be chosen to account for the solution chemistry of the metal ion, including solubility, redox and hydrolysis, as well as the properties of the biological macromolecule. This may involve the choice of pH, buffer, ionic strength, a competing ligand, and even solvent that are optimal for the binding reaction of interest.

2. The buffer needs to be chosen not only for maintaining the desired pH but also for its interaction with the metal, unless a more strongly binding ligand is also present. Metal-buffer contributions to the net binding constant and enthalpy must be subtracted, so stability constants [12] and formation enthalpies of metal-buffer complexes need to be available [9] or determined [13].

3. The choice of concentrations depends on practical considerations (e.g., protein solubility) and the need for a measurable amount of heat with each aliquot, as well as the concentration dependence of the c window. Since heat is an extrinsic property, higher protein concentrations will increase the signal. When $\Delta C_p°$ is not negligible, $\Delta H°$ will vary with temperature and, depending on the sign of $\Delta C_p°$, a lower or higher temperature will increase the measurable heat. In addition, since metals often displace protons upon binding to protein residues, a buffer with a larger heat of protonation may amplify the net signal (see below).

4. The number and stoichiometry of binding events may be obvious from inflections in the ITC data. However, resolving the thermodynamics of multiple binding events is often challenging, and prior knowledge of the binding stoichiometry reduces the number of fitting parameters, which is crucial for low affinity cases [6].

5. When a titration involves more than one binding event, data obtained from the corresponding reverse titration (macromolecule → metal) can be particularly valuable. These data provide the reciprocal stoichiometry, and the initial aliquots have a different component in large excess. Higher confidence in the binding thermodynamics is achieved when a single set of parameters is able to fit both the forward and reverse titrations [14].

6. The unavoidable heat of dilution of the species in the syringe needs to be determined and subtracted from each injection. The dilution heat should be kept to a minimum by matching the pH, buffer, ionic strength and concentrations (except for the two binding species) of the solutions in the syringe and cell as closely as possible. This heat is determined either through a separate background titration that lacks the macromolecule in the reaction cell (Note, subtraction of this control titration does not account for the metal-buffer interaction) or by extending the titration

until a constant background heat is measured. The latter method is generally preferred because it measures the dilution heat for the exact experimental conditions. However, evidence for metal hydrolysis may be found in a background dilution titration, where a signal that is highly dependent on concentration would indicate a competing hydrolysis reaction.

7. Multiple titrations are usually required to find optimal experimental conditions. Sometimes it may be desirable to use concentrations and injection volumes that accentuate earlier or later portions of the titration [15], which may require the concatenation of two or more syringes of titrant [13, 14, 16]. Unless ITC is only being used to measure the binding enthalpy, the isotherm needs to fall within the c window. When the protein has a high affinity for the metal, the stability constant can be determined by introducing a known competing ligand, L_C, which results in a lower experimental K_{ITC} and a lower c value. When L_C is present in both the syringe and the cell in sufficient excess that its concentration is essentially constant during the titration, as is the case for the buffer, then a simple relationship exists between K_{ITC} and the desired $K_{MProtein}$, as derived below for L_C = buffer. However, when L_C is not present in excess and its concentration changes during the titration, then analysis of the binding isotherm is more complex, as noted below.

8. After subtracting the heat of dilution, ITC data are fit to one or more binding models to determine the net thermodynamic values. Common fitting models include the one site, the two or three [17] independent sites, the multiple sequential sites and the competition [18] model. In addition, functions for more complex binding equilibria can be developed and used to fit the data. The 'goodness of fit' is typically indicated by the χ^2 value, which is one parameter that can be used to compare different binding models when investigating the binding mechanism. However, the number of independent variables (degrees of freedom) for each model needs to be considered and the data must justify the use of a more complex model with more adjustable parameters.

9. As with any quantitative measurement, an estimate of the error in the reported values requires a statistical analysis of the best-fit values from two or more reproducible data sets collected under conditions that optimize precision [19]. Fitting software typically calculates the standard deviation for the fit parameters, but these errors from individual data sets are generally smaller than the standard deviations from multiple ITC measurements.

10. ITC has the ability to quantify the number of protons that are transferred (typically displaced) upon metal binding [20, 21]. This requires ΔH_{ITC} values at the same pH in two or more buffers with different protonation enthalpies. However, the enthalpy of metal-buffer interaction must also be included in this analysis [13, 15]. Conversely, metal binding data at different pH's can be used to determine pK_a's associated with coupled proton transfer [20, 21].

Data Analysis

Models for fitting ITC data typically involve one or more independent binding sites or sequential binding to multiple sites. Choice of the fitting model is guided by the data and prior knowledge about the binding stoichiometry. When the metal (M) and ligand (L) form a 1:1 complex and no other equilibria are involved, then all of the measured heat is due to the equilibrium of interest (Eq 1),

$$M + L \rightleftarrows ML \tag{1}$$

and a simple fitting algorithm for this one-site model is derived from equations 2-4.

$$C_M = [ML] + [M] \tag{2}$$

$$C_L = [ML] + [L] \tag{3}$$

$$K_{ITC} = \frac{[ML]}{[M][L]} \tag{4}$$

However, when multiple metal and/or ligand species and competing equilibria are involved, as is commonly the case with metals and proteins, then further analysis is required to determine the binding constants and enthalpies of interest from the experimental values, K_{ITC} and ΔH_{ITC}. These condition-dependent values contain multiple contributions and are only comparable to other values determined under *identical* conditions. Outlined below is a procedure to obtain condition-independent thermodynamic values from the average best-fit experimental ITC values. In this example the metal can form a 1:1 complex with the buffer, B,

and the ligand (protein) exists in three protonation states (L, HL$^+$ and H$_2$L^{2+}) at the experimental pH. The overall equilibrium is given by equation 5.

$$(1\text{-}\alpha_{MB})M + \alpha_{MB}MB + (1\text{-}\alpha_{HL}\text{-}\alpha_{H2L})L + \alpha_{HL}HL^+ + \alpha_{H2L}H_2L^{2+} \rightleftharpoons ML + (\alpha_{HL}+2\alpha_{H2L})HB^+ + (\alpha_{MB}\text{-}\alpha_{HL}\text{-}2\alpha_{H2L})B \quad (5)$$
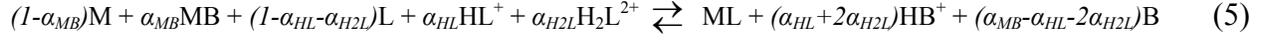
More complex situations involving additional speciation and/or multiple binding equilibria are analysed by extensions of the analysis for this simple case.

1. Equilibrium Constant

The overall equilibrium includes two competing equilibria that could be found with metal complexation in a buffered aqueous solution, buffer competition with the ligand for the metal and proton competition with the metal for the ligand. To account for the additional species and their coupled equilibria, equations 2 and 3 need to be rewritten as equations 6 and 7, respectively, and equations 8-11 must be considered.

$$C_M = [M] + [MB] + [ML] \quad (6)$$

$$C_L = [L] + [HL^+] + [H_2L^{2+}] + [ML] \quad (7)$$

$$K_{MB} = \frac{[MB]}{[M][B]} \quad (8)$$

$$K_{HL} = \frac{[HL^+]}{[H^+][L]} = K_{a1}^{-1} \quad (9)$$

$$K_{2,H_2L} = \frac{[H_2L^{2+}]}{[HL^+][H^+]} = K_{a2}^{-1} \quad (10)$$

$$K_{ML} = \frac{[ML]}{[M][L]} \quad (11)$$

Equation 12 is also introduced at this point.

$$\beta_{2,H_2L} = K_{HL}K_{2,H_2L} = \frac{[H_2L^{2+}]}{[L][H^+]^2} = K_{a1}^{-1}K_{a2}^{-1} \quad (12)$$

Equation 4 for the simple case now becomes equation 13 for this more complex situation,

$$K_{ITC} = \frac{[ML]}{[M]_{ITC}[L]_{ITC}} \tag{13}$$

where $[M]_{ITC}$ and $[L]_{ITC}$ indicate the metal and ligand species not in the ML complex, as defined by equation 14 (based on equations 6 and 8),

$$[M]_{ITC} = C_M - [ML] = [M] + [MB] \tag{14a}$$

$$[M]_{ITC} = [M](1 + K_{MB}[B]) = \alpha_{Buffer}[M] \tag{14b}$$

where $\alpha_{Buffer} = 1 + K_{MB}[B]$, and equation 15 (based on equations 7, 9 and 12),

$$[L]_{ITC} = C_L - [ML] = [L] + [HL^+] + [H_2L^{2+}] \tag{15a}$$

$$[L]_{ITC} = [L](1 + K_{HL}[H^+] + \beta_{2,H2L}[H^+]^2) = \alpha_{Proton}[L] \tag{15b}$$

where $\alpha_{Proton} = 1 + K_{HL}[H^+] + \beta_{2,H2L}[H^+]^2$.

Substituting equations 14b and 15b into equation 13 gives,

$$K_{ITC} = \frac{[ML]}{[M][L]} * \frac{1}{\alpha_{Proton}\alpha_{Buffer}} = \frac{K_{ML}}{\alpha_{Proton}\alpha_{Buffer}} \tag{16}$$

which finally leads to an expression (Eq 17) for the desired K_{ML},

$$K_{ML} = \alpha_{Proton}\alpha_{Buffer}K_{ITC} = K_{ITC}\left(1 + K_{HL}[H^+] + \beta_{2,H_2L}[H^+]^2\right)\left(1 + K_{MB}[B]\right) \tag{17}$$

where K_{ITC} is obtained from a fit of the ITC isotherm, and α_{Proton} and α_{Buffer} account for proton and buffer competition, respectively. This expression indicates how the concentrations of competing species (proton, buffer) and the magnitudes of equilibria involving these species (K_{HL}, $\beta_{2,H2L}$, K_{MB}) affect the experimental binding constant, K_{ITC}. Related expressions are readily derived for α_{Proton} and α_{Buffer} that account for different metal-buffer species (e.g., 1:2 complex) and ligand protonation states.

To verify the accuracy of this analysis to determine the pH- and buffer-independent binding constant K_{ML} from the experimental K_{ITC}, functions that account for the coupled equilibria and determine K_{ML} directly from experimental data were derived (Supplementary Material) [22]. The solver function of Excel®, with standard χ^2 minimization and error evaluation [23], was then used to fit ITC data with this coupled-equilibria model. Figure 3 shows representative ITC data for Zn^{2+} binding to trien (triethylenetetramine) in Tris buffer, and the best fit of these data with the Origin® one-site model and with this Excel® coupled-equilibria model that accounts for the four trien pK_a values and the Zn^{2+}-Tris complex. As observed, excellent fits to the experimental data are obtained with both models.

Several ITC data sets with different metals, buffers and ligands have been fit with three models, the one-site model available in Origin®, an analogous one-site model that is based on equations 2-4 and written in Excel®, and the model indicated above that is written in Excel® and directly accounts for the coupled buffer and protonation equilibria [22]. Table 1 compares the best-fit values for these data sets with the three models. The initial sets are for Zn^{2+} binding to trien and provide an ideal case because K_{ITC} falls in the middle of the c window for a variety of experimental (buffer, pH) conditions. The second group of data sets consists of different metal ions binding to a short histidine-rich peptide [13], which also has four relevant pK_a's and forms 1:1 metal complexes with a somewhat lower metal affinity. In all cases, good to excellent agreement is found between the best-fit parameters obtained with the two one-site models, validating the Excel®-based fitting procedure. The last column in Table 1 indicates the log K_{ML} values that are obtained from an analysis of the Origin® one-site K_{ITC} values (first column) using a relationship that is analogous to equation 17 and accounts for the four ligand pK_a values and the metal-buffer complex. Excellent agreement is found between these log K_{ML} values and those

obtained with the Excel®-based fitting model that includes the coupled equilibria (third column).

Thus, the analysis of K_{ITC} based on equation 17 and similar relationships accurately accounts for

buffer and proton competition in metal-binding ITC data and provides a simple method to obtain

the buffer- and pH-independent binding constants.

When there is an additional competing species whose free concentration changes

significantly during the titration, the ITC data must be fit with an analysis that accounts for the

competing equilibrium and changing concentration. For the case of one species (A) displacing

another species (B) that is initially bound to a protein (i.e., A → protein-B), a competition fitting

model has been developed by Sigurskjold [18]. Recently this analysis and fitting has been

extended to the case where a metal that is initially in a complex of known stability with a

competing ligand (L_C) is titrated into a protein solution (i.e., M(L_C)$_n$ → protein) [24]. The

competing ligand will eliminate metal-buffer interaction but buffer protonation will still

contribute to ΔH_{ITC} if proton transfer (displacement) accompanies metal binding.

2. Enthalpy

All equilibria that contribute to the experimental binding constant, K_{ITC}, also contribute

to the net measured heat, ΔH_{ITC}. Hess's Law is used to decompose this experimental value into

the individual contributions to determine the desired $\Delta H°_{ML}$. Table 2 contains the individual

equilibria that contribute to the overall equilibrium (Eq 5), as well as the coefficients that

indicate the percentage of the metal and ligand species in solution under the experimental

conditions. These are determined (Eqs 18-20) from equations 6-10 and 12, and setting [ML] = 0.

$$\alpha_{MB} = \frac{[MB]}{C_M} = \frac{K_{MB}[B]}{\alpha_{Buffer}} \tag{18}$$

$$\alpha_{HL} = \frac{[HL^+]}{C_L} = \frac{K_{HL}[H^+]}{\alpha_{Proton}} \tag{19}$$

$$\alpha_{H2L} = \frac{\left[H_2 L^{2+}\right]}{C_L} = \frac{\beta_{2,H_2L}\left[H^+\right]^2}{\alpha_{Proton}} \tag{20}$$

Equation 21, which is based on Hess's Law, is now rearranged to solve for $\Delta H°_{ML}$.

$$\Delta H_{ITC} = -\alpha_{MB}\Delta H°_{MB} - \alpha_{HL}\Delta H°_{HL} - \alpha_{H2L}\Delta H°_{H2L} + (\alpha_{HL}+2\alpha_{H2L})\Delta H°_{HB} + \Delta H°_{ML} \tag{21}$$

Finally, standard thermodynamic expressions are used to determine $\Delta G°_{ML}$ and $\Delta S°_{ML}$

from the values of K_{ML} and $\Delta H°_{ML}$ obtained from this analysis of the ITC data.

3. Proton Competition

When proton transfer (typically proton displacement) accompanies metal binding, it may

not be possible to account for protonation/deprotonation contributions to K_{ITC} and ΔH_{ITC} *a*

priori. However, the number of protons that are involved at a given pH can be determined

experimentally by the buffer protonation (or deprotonation) contribution to ΔH_{ITC}. Equation 22,

$$\Delta H_{ITC} = n_{H+}(\Delta H°_{HB} - \Delta H°_{HL}) + \Delta H°_{ML} - \Delta H°_{MB} \tag{22}$$

which is a somewhat simplified version of equation 21, indicates the relationship between ΔH_{ITC}

and $\Delta H°_{HB}$. It shows that a plot of $(\Delta H_{ITC} + \Delta H°_{MB})$ vs. $\Delta H°_{HB}$ for data collected at the same pH

in two or more buffers with different protonation enthalpies has a slope corresponding to n_{H+}

$(\alpha_{HL}+2\alpha_{H2L}$ in Eq 5, for the case described above), the number of protons transferred. Unique to

titrations involving metals is the enthalpy of formation of the metal-buffer complex, $\Delta H°_{MB}$,

which will also vary with the buffer and must be included in this analysis. The intercept of this

plot, $\Delta H°_{ML} - n_{H+}\Delta H°_{HL}$, indicates the net enthalpy associated with metal binding and

displacement of protons from the ligand (protein binding site).

4. Heat Capacity

The change in heat capacity associated with metal binding is determined from the temperature-

dependence of the binding enthalpy, $\Delta C_p° = \Delta\Delta H°/\Delta T$. However, analysis that is based on the

experimental ΔH_{ITC} will include contributions to $\Delta C_p°$ from the enthalpies of metal-buffer complex formation and buffer protonation, which may also depend on temperature. For example, we have measured $\Delta C_p° = 17.4 \pm 0.7$ cal/mol•K for the protonation of Tris. Ideally, a Hess's Law analysis (see Table 2) should be used to determine $\Delta H°_{ML}$ at each temperature to determine $\Delta C_p°$ for the metal binding to the ligand (protein). At the minimum, this analysis should subtract the contributions to $\Delta C_p°$ from coupled equilibria involving the buffer by removing both $\Delta H°_{MB}$ and $\Delta H°_{HB}$ contributions to ΔH_{ITC} (Eq 22) at each temperature. Quantification of $\Delta H°_{HB}$, though, requires the number of protons that are displaced, n_{H+}, at the experimental pH.

Summary

Isothermal titration calorimetry (ITC) can be used to quantify the thermodynamics of metal ions binding to proteins and other biological molecules. However, potentially competing reactions (e.g., precipitation, hydrolysis, redox) and commonly coupled equilibria (metal-buffer interaction, proton competition) are well known for metals. This requires experimental conditions to avoid the former and subsequent data analysis to account for the latter and their contributions to the experimental K_{ITC} and ΔH_{ITC} values. To determine the condition-independent binding constant, K_{ML}, metal and ligand (protein) species that are present in the experimental solution must be known, and K_{ITC} is analyzed with an appropriate expression for K_{ML} (e.g., Eq 17) that accounts for coupled equilibria involving these species. The condition-independent binding enthalpy, $\Delta H°_{ML}$, is determined with a simple Hess's Law analysis of ΔH_{ITC}, which requires the enthalpies of coupled equilibria and the number of protons that are transferred (typically displaced) upon metal binding. The latter is experimentally quantified by the contribution of buffer protonation enthalpy to ΔH_{ITC}. Multiple binding parameters (e.g., K_{ML}

and $\Delta H°_{ML}$) may be determined simultaneously with appropriate software, such as HypDH [26], that can account for coupled equilibria in fits of the experimental ITC isotherms. Finally, the condition-independent values of K_{ML} and $\Delta H°_{ML}$ are used to determine the binding free energy $\Delta G°_{ML}$ and entropy $\Delta S°_{ML}$. In addition, the temperature dependence of $\Delta H°_{ML}$ allows the change in heat capacity, $\Delta C_p°$, associated with metal binding to be determined. Although the experimental concerns and data analysis for ITC measurements involving metal ions may appear somewhat daunting, careful experiments and analysis of the data are required to obtain accurate condition-independent thermodynamic values.

References

1. Wiseman T, Williston S, Brandts JF, Lin L (1989) Anal Biochem 179:131-137

2. Freire E, Mayorga OL, Straume M (1990) Anal Chem 62:950A-959A

3. http://www.microcal.com/reference-center/reference-list.asp

4. Wilcox DE (2008) Inorg Chim Acta 361:857-867

5. Connors KA (1987) Binding Constants, the Measurement of Molecular Complex Stability. Wiley, New York

6. Turnbull WB, Daranas AH (2003) J Am Chem Soc 125:14859-14866

7. Lin LN, Mason AB, Woodworth RC, Brandts JF (1991) Biochemistry 30:11660-11669

8. Lin LN, Mason AB, Woodworth RC, Brandts JF (1993) Biochemistry 32:9398-9406

9. NIST Standard Reference Database 46; Critically Selected Stability Constants of Metal Complexes: version 8.0 (2004)

10. Krezel A, Lesniak W, Jezowska-Bojczuk M, Mlynarz P, Brasun J, Kozlowski H, Bal W (2001) J Inorg Biochem 84:77-88

11. Krezel A, Latajka R, Bujacz GD, Bal W (2003) Inorg Chem 42:1994-2003

12. Magyar JS, Godwin HA (2003) Anal Biochem 320:39-54

13. Grossoehme NE, Akilesh S, Guerinot ML, Wilcox DE (2006) Inorg Chem 45:8500-8508

14. Spuches AM, Kruszyna HG, Rich AM, Wilcox DE (2005) Inorg Chem 44:2964-2972

15. Grossoehme NG, Mulrooney SB, Hausinger RP, Wilcox DE (2007) Biochemistry 46:10506-10516

16. Bou-Abdallah F, Arosio P, Santambrogio P, Yang X, Janus-Chandler C, Chasteen ND (2002) Biochemistry 41:11184-11191

17. Bou-Abdallah F, Woodhall MR, Velazquez-Campoy A, Andrews SC, Chasteen ND (2005) Biochemistry 44:13837-13846

18. Sigurskjold BW (2000) Anal Biochem 277:260-266

19. Tellinghuisen J (2005) J Phys Chem B 109:20027-20035

20. Doyle ML, Louie G, Dal Monte PR, Sokoloski TD (1995) Meth Enzymol 259:183-194

21. Baker BM, Murphy KP (1996) Biophys J 71:2049-2055

22. Grossoehme NG (2007) PhD thesis, Dartmouth College

23. Billo EJ (2001) Excel for Chemists: A Comprehensive Guide (2nd Ed). Wiley-VCH, New York

24. Hong L, Bush WD, Hatcher LQ, Simon J (2008) J Phys Chem B 112:604-611

25. Eide D, Broderius M, Fett J, Guerinot ML (1996) Proc Natl Acad Sci USA 93:5624-5628

26. Gans P, Sabatini A, Vacca A (2008) J Solution Chem 37:467-476

Experiment		Origin 1-site			Excel 1-site			Excel H$_4$L-MB			Log K$_{ML}$
						Fitting Model					
A. trien[a]											
Zn^{2+} → trien 25 mM ACES, pH 7.25 log β_{MB2} = 3.74	log K	5.53	±	0.04	5.50	±	0.08	**11.02**	±	0.09	**11.19**
	ΔH	1.21	±	0.01	1.20	±	0.03	1.20	±	-	
	n	1.05	±	0.01	1.05	±	0.01	1.05	±	-	
Zn^{2+} → trien 100 mM Tris, pH 7.45 log K$_{MB}$ = 2.27	log K	6.04	±	0.03	6.04	±	0.04	**10.72**	±	0.04	**10.67**
	ΔH	-5.61	±	0.04	-5.31	±	0.05	-5.31	±	-	
	n	0.99	±	0.01	0.96	±	0.01	0.96	±	-	
Zn^{2+} → trien 100 mM Tris, pH 8.1 log K$_{MB}$ = 2.27	log K	6.48	±	0.02	6.53	±	0.02	**10.37**	±	0.02	**10.22**
	ΔH	-6.19	±	0.02	-5.84	±	0.02	-5.84	±	-	
	n	1.01	±	0.01	0.99	±	0.01	0.99	±	-	
Zn^{2+} → trien 25 mM MOPS, pH 7.25 log K$_{MB}$ = 3.22	log K	6.05	±	0.05	6.08	±	0.07	**11.71**	±	0.07	**11.67**
	ΔH	3.12	±	0.03	3.00	±	0.04	3.00	±	-	
	n	0.98	±	0.01	0.96	±	0.01	0.96	±	-	
B. IRT1pep[b]											
Fe^{2+} → IRT1pep 25 mM MOPS, pH 7.25 log K$_{MB}$ = 1.14	log K	2.6	±	0.4	2.3	±	0.4	**2.84**	±	0.03	**2.86**
	ΔH	-3.48	±	0.14	-5.4	±	0.2	-5.4	±	-	
	n	1	±	-	1	±	-	1	±	-	
Cu^{2+} → IRT1pep 25 mM ACES, pH 7.25 log β_{MB2} = 7.77	log K	4.4	±	0.4	4.2	±	0.4	**7.87**	±	0.01	**7.88**
	ΔH	-5.1	±	0.1	-5.5	±	0.3	-5.5	±	-	
	n	0.99	±	0.04	0.95	±	0.03	0.95	±	-	
Zn^{2+} → IRT1pep 25 mM ACES, pH 7.25 log β_{MB2} = 3.74	log K	3.9	±	0.4	3.8	±	0.4	**5.55**	±	0.02	**5.54**
	ΔH	-2.97	±	0.06	-3.32	±	0.08	-3.32	±	-	
	n	1.3	±	0.2	1.3	±	0.1	1.3	±	-	
Cd^{2+} → IRT1pep 25 mM ACES, pH 7.25 log β_{MB2} = 2.96	log K	3.6	±	0.4	3.4	±	0.4	**4.88**	±	0.06	**4.84**
	ΔH	-6.39	±	0.08	-7.8	±	0.4	-7.8	±	-	
	n	1.01	±	0.04	0.9	±	0.1	0.9	±	-	

Table 1. Best fit values, and associated error, from fitting the indicated experimental ITC data to three models (see text); absence of an error indicates that the value was fixed; [a] trien pK$_a$ values are 3.27, 6.58, 9.07 and 9.75 [9]; [b] IRT1pep is the N-acetylated and C-amidated peptide PHGHGHGHGP that corresponds to this sequence in the large intracellular loop of the membrane metal transport protein IRT1 from *Arabidopsis thaliana* [25]; data are from Ref 13, where the IRT1pep pK$_a$ values were determined to be 3.4, 5.3, 6.7 and 7.4.

	Reaction[a]	Coefficient	ΔH^{b}
1	$MB \rightleftharpoons M + B$	α_{MB}	$-\Delta H^{\circ}_{MB}$
2	$HL^{+} \rightleftharpoons L + H^{+}$	α_{HL}	$-\Delta H^{\circ}_{HL}$
3	$H_2L^{2+} \rightleftharpoons L + 2H^{+}$	α_{H2L}	$-\Delta H^{\circ}_{H2L}$
4	$M + L \rightleftharpoons ML$	1	ΔH°_{ML}
5	$B + H^{+} \rightleftharpoons HB^{+}$	$\alpha_{HL} + 2\alpha_{H2L}$	ΔH°_{HB}
6	$(1-\alpha_{MB})M + \alpha_{MB}MB + (1-\alpha_{HL}-\alpha_{H2L})L + \alpha_{HL}HL^{+} + \alpha_{H2L}H_2L^{2+} \rightleftharpoons$ $ML + (\alpha_{HL}+2\alpha_{H2L})HB^{+} + (\alpha_{MB}-\alpha_{HL}-2\alpha_{H2L})B$	1	ΔH_{ITC}

Table 2. Individual equilibria (1-5) that contribute to the experimental equilibrium (6) involving a metal (M) binding to a ligand (L) found in three protonation states at the experimental pH that is maintained by a buffer (B); [a] equilibria are written in the direction that the reaction occurs (1-3 are dissociations, 4-5 are associations); [b] ΔH° values are for the association reactions.
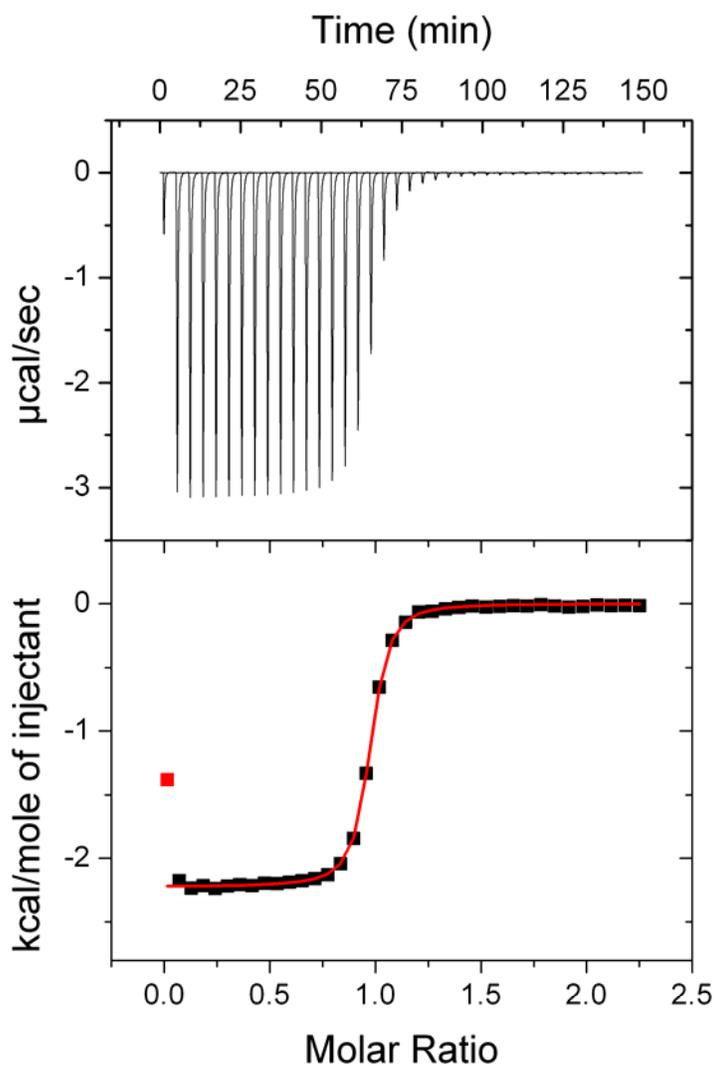
Figure 1. Representative ITC data for $Mg^{2+} \rightarrow$ EDTA in 50 mM Tris, pH 8.1 and 100 mM NaCl at 25°C; top panel is the raw baseline-smoothed ITC data plotted as heat flow vs. time, while the bottom panel is the integrated and concentration-normalized heat for each injection verses the Mg^{2+}-to-EDTA molar ratio; non-linear least squares analysis of the data in the bottom panel with the Origin® one-site model gives the best fit values $n = 0.95 \pm 0.01$, $K_{ITC} = 1.02 \pm 0.01 \times 10^6$ and $\Delta H_{ITC} = -2.22 \pm 0.02$ kcal/mol.
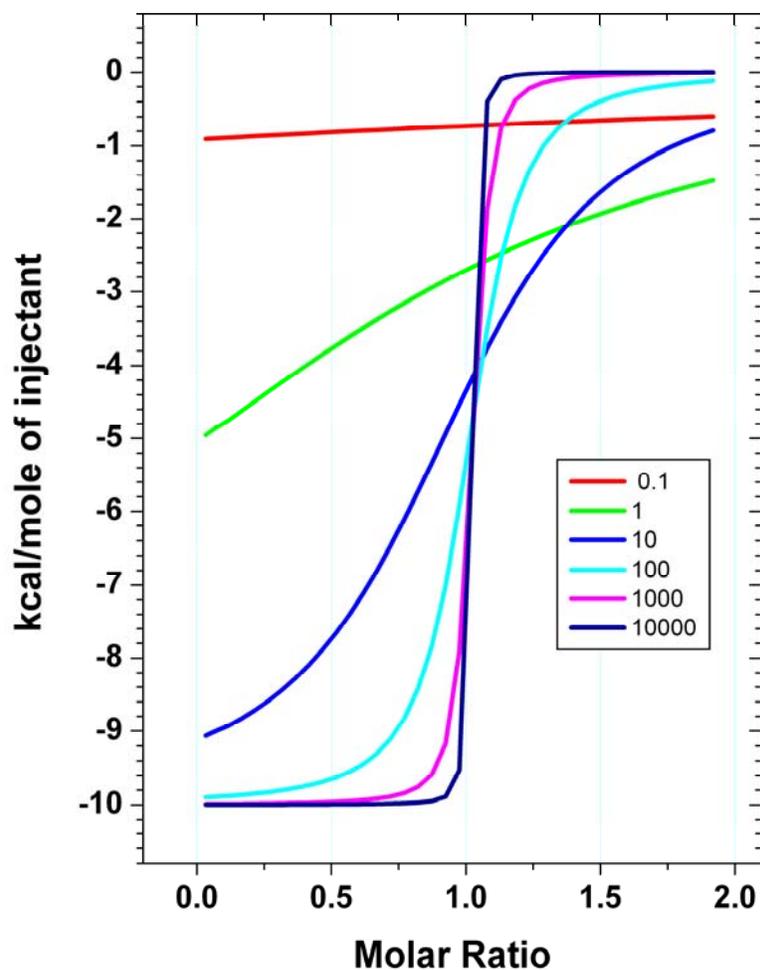
Figure 2. Theoretical ITC isotherms generated with the Origin® one-site fitting model and different values of c (inset) using the parameters $n = 1$, $\Delta H = -10$ kcal/mol and [macromolecule] = 0.1 mM, and varying K from 1×10^3 to 1×10^8; with this macromolecule concentration, a unique fit could be achieved in the range $\sim 1 \times 10^4 < K < \sim 1 \times 10^7$.
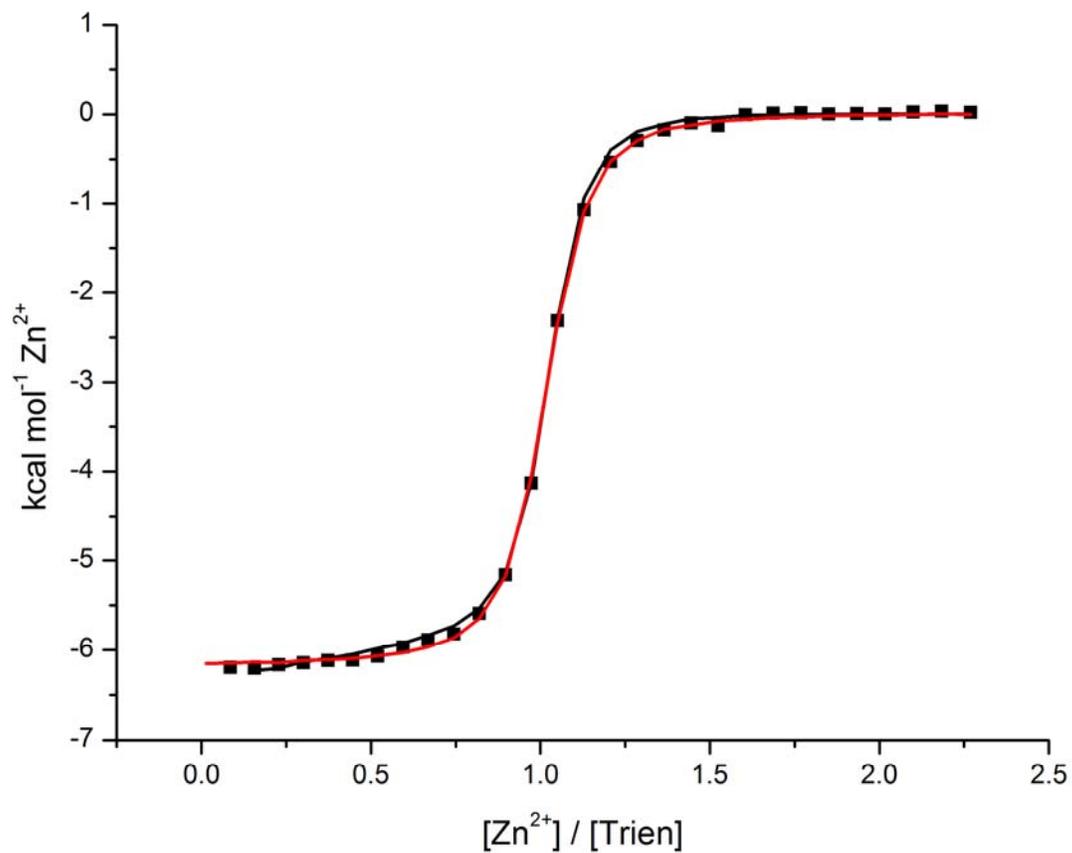
Figure 3. Integrated heats from a 0.90 mM Zn^{2+} → 0.090 mM trien titration in 100 mM Tris, pH 8.1 at 25°C; best fit to the Origin® one-site model (red line) and the Excel® model that accounts for coupled equilibria (black line) are indicated; best-fit parameters are indicated in Table 1.